Journal of ELECTRONIC MATERIALS, Vol. 44, No. 1, 2015
DOI: 10.1007/s11664-014-3448-z

Interfacial Reactions Between Cu-Ag Alloy Substrates and Sn

TENG-KAI YANG,[1] CHIH-FAN LIN,[1] and CHIH-MING CHEN[1,2,3]

1.—Department of Chemical Engineering, National Chung Hsing University, 250, Kuo Kuang Road, Taichung 402, Taiwan. 2.—e-mail: chencm@dragon.nchu.edu.tw. 3.—e-mail: chencm@nchu.edu.tw

Interfacial reactions between Sn and Cu-*x*Ag alloys (x = 0 at.%, 11.1 at.%, 33.3 at.%, and 50 at.%) were investigated. The as-prepared Cu-Ag alloys displayed a microstructure composed of a proeutectic (Cu) phase and a eutectic (Cu) + (Ag) structure, where the fraction of the eutectic structure increased with increasing Ag content. At 200°C and 250°C, reactions to form Cu_6Sn_5 and Cu_3Sn phase occurred at the Sn/Cu-Ag interface, and also inside the Cu-Ag substrate along the (Ag)/(Cu) interphase interface. The penetrated growth behavior by way of the (Ag)/(Cu) interphase interface accelerated the growth rate of the intermetallic compounds and the consumption of the Cu-Ag substrates. A comparison between conventional Sn/Cu and Sn/Cu-Ag systems indicated that addition of Ag to Cu had a significant accelerating effect on the Sn/Cu-*x*Ag interfacial reaction to form Cu_6Sn_5.

Key words: Intermetallic compounds, Cu, Ag, interphase interface

INTRODUCTION

Due to environmental protection and human health concerns, lead-free Sn-based alloys have widely replaced conventional Sn-Pb alloys as solder materials in the electronics packaging industry.[1,2] This replacement caused not only comprehensive remodulation/reoptimization of the processing parameters but also certain new reliability issues. One such issue resulted from the high Sn content in lead-free solders, potentially causing excessive growth of brittle intermetallic compounds at the solder/substrate interfaces of solder joints; For example, eutectic or near-eutectic Sn-Ag, Sn-Cu, and Sn-Ag-Cu solders contain over 95 wt.% Sn. Use of these solders on common Cu substrates subjected to high-temperature aging results in excessive growth of Cu_6Sn_5 and Cu_3Sn phases and consumes significant amounts of the Cu substrate.[2–5] Kirkendall voids might also accompany the Cu_3Sn phase growth and mechanically weaken the solder joints.[6–8] One feasible solution to these problems is to add a third or fourth element to such high-Sn lead-free solders[9,10] to manipulate the intermetallic compound formation/growth at solder joints.

This alloying strategy using minor elemental additions to solders was also feasible for Cu substrates.[11,12] Yu et al. added 15 wt.% to 30 wt.% Zn to a Cu substrate and found that the growth of both Cu_6Sn_5 and Cu_3Sn was suppressed.[13] Furthermore, Kirkendall voids were also significantly inhibited. Zhang's group found that adding Ag (2.5 at.% and 18.7 at.%), Al (2.3 at.%), Sn (3 at.%), and Zn (10 at.%) to Cu substrate effectively improved the mechanical reliability by eliminating interfacial embrittlement at SnBi/Cu-X (X = Ag, Al, Sn, Zn) joints induced by Bi segregation.[12,14] Those authors suggested that Bi atoms diffused into the Cu-X substrate instead of segregating at the joint interface. Zou et al. added Ag, Sn, and Zn to Cu substrate and investigated the interfacial microstructures for Sn-4 wt.%Ag/Cu-X couples.[11] They found that adding Ag and Zn effectively suppressed the Cu_3Sn growth, but the opposite effect was observed after adding Sn to the Cu. Lai et al. investigated the wetting behavior of molten Sn on a Cu-Fe two-phase composite under high vacuum at 400°C.[15] Enhanced wetting was observed and attributed to the interfacial microroughness caused by the inconsistent dissolution of the Fe and Cu phases.

(Received March 25, 2014; accepted September 24, 2014; published online October 15, 2014)

This study focused on the effects of alloying the Cu substrate with Ag on the solder/Cu interfacial reactions. Three Ag-containing Cu substrates, namely Cu-11.1Ag, Cu-33.3Ag, and Cu-50Ag (in at.%), were used to systematically investigate the effects of the Ag content. The experimental results indicated that the Ag content affected the Cu-Ag substrate microstructure and the interfacial reactions between the Cu-Ag and pure Sn solder.

EXPERIMENTAL PROCEDURES

Pure Sn pieces (99.8%; Showa, Japan) were hammered into plates and sequentially cleaned in dilute (5%) H_2SO_4, acetone, and deionized water. The Sn plate was placed on a slide after coating with a tiny flux (Magana 51 flux, USA). The slide and Sn plate were placed on a hot plate at 250°C. The Sn plate melted and became a molten ball due to surface tension. The Sn ball solidified naturally in air after removal from the hot plate and was used as the solder material. Three Ag-alloyed Cu substrates were prepared: Cu-11.1Ag, Cu-33.3Ag, and Cu-50Ag. First, the appropriate weights of pure Ag (99.9%; Alfa Aesar, USA) and Cu (99.5%; Alfa Aesar, USA) shots were sealed in a vacuum quartz tube. Then, the quartz tube was placed in a tube furnace at 1200°C. The Ag and Cu shots melted and mixed to form a molten alloy in the quartz tube. To ensure that the as-prepared Cu-Ag alloy was homogeneous, the quartz tube was shaken several times before the alloy solidified. After a 72-h heat treatment, the furnace was turned off, and the sample cooled naturally in the furnace. The solidified Cu-Ag ingot was removed from the quartz tube and cut into 1-mm-thick disks using a diamond saw. A polyimide film with a circular opening (2 mm diameter) covering the Cu-Ag substrate was used to control the reaction area between the solder and Cu-Ag substrate. The uncovered Cu-Ag surface was coated with a tiny flux to assist the reaction between the solder and Cu-Ag substrate.

The Sn solder ball was placed on the Cu-Ag substrate, which was then placed on a hot plate set to 250°C. The liquid/solid interfacial reaction between the Sn and solid Cu-Ag substrate occurred once the Sn ball became molten. The reaction time was set from 1 min to 30 min. Solid/solid interfacial reactions were also performed. First, the liquid/solid interfacial reaction mentioned above was performed for 1 min to join the Sn and Cu-Ag. Then, the joined Sn/Cu-Ag samples were placed in an oven at 200°C for 24 h to 240 h. Reference liquid/solid and solid/solid interfacial reactions were also performed using the pure Sn/pure Cu system to investigate the effects of adding Ag to the Cu substrate.

After these reactions, the samples were removed from the hot plate or oven and mounted in epoxy resin for metallographic examination. The samples were ground and polished perpendicular to the Sn/Cu-Ag interface using sandpaper and Al_2O_3 powder, respectively. Scanning electron microscopy (SEM) was used to observe the cross-sectional microstructure of the Sn/Cu-Ag interface. Compositional analysis was performed using energy-dispersive

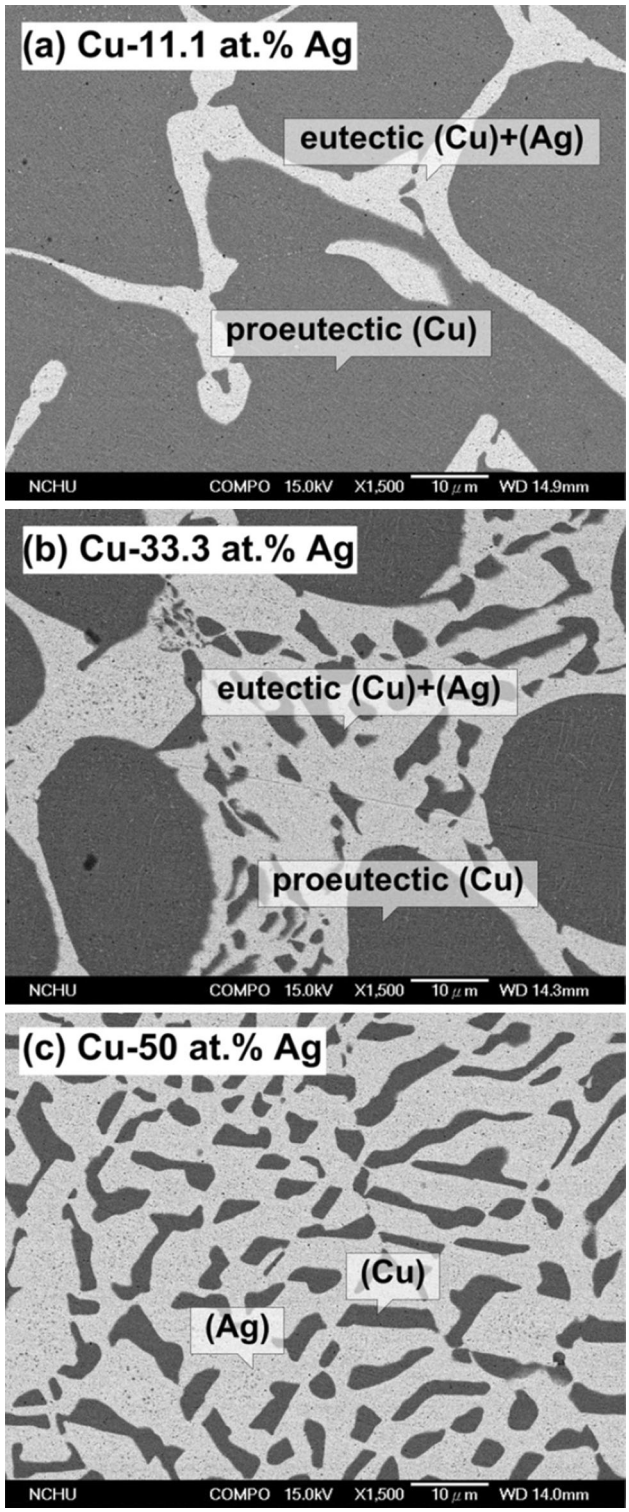

Fig. 1. SEM micrographs showing the microstructures of three as-solidified Cu-Ag alloys: (a) Cu-11.1 at.%Ag, (b) Cu-33.3 at.%Ag, and (c) Cu-50 at.%Ag.

x-ray (EDX) spectrometry. An image processing system was used to measure the intermetallic compound thicknesses.

RESULTS AND DISCUSSION

Microstructures of As-Solidified Cu-Ag Substrates

Figure 1 shows SEM micrographs of the three solidified Cu-Ag alloy microstructures. The microstructural evolution of the Cu-Ag alloys can be explained based on the Cu-Ag binary phase diagram.[16] The Cu-Ag alloy is a simple eutectic system, and the three Cu-Ag alloy compositions prepared in this study are located in the hypereutectic region. During solidification, a proeutectic (Cu) phase formed first, and the rest of the liquid phase transformed into a eutectic structure consisting of (Cu) and (Ag) as the temperature decreased below the eutectic temperature. According to the EDX analysis, the dark phase in Fig. 1 was Cu rich with a small amount of dissolved Ag and was identified as the (Cu) phase. The bright phase was Ag rich with a small amount of dissolved Cu,

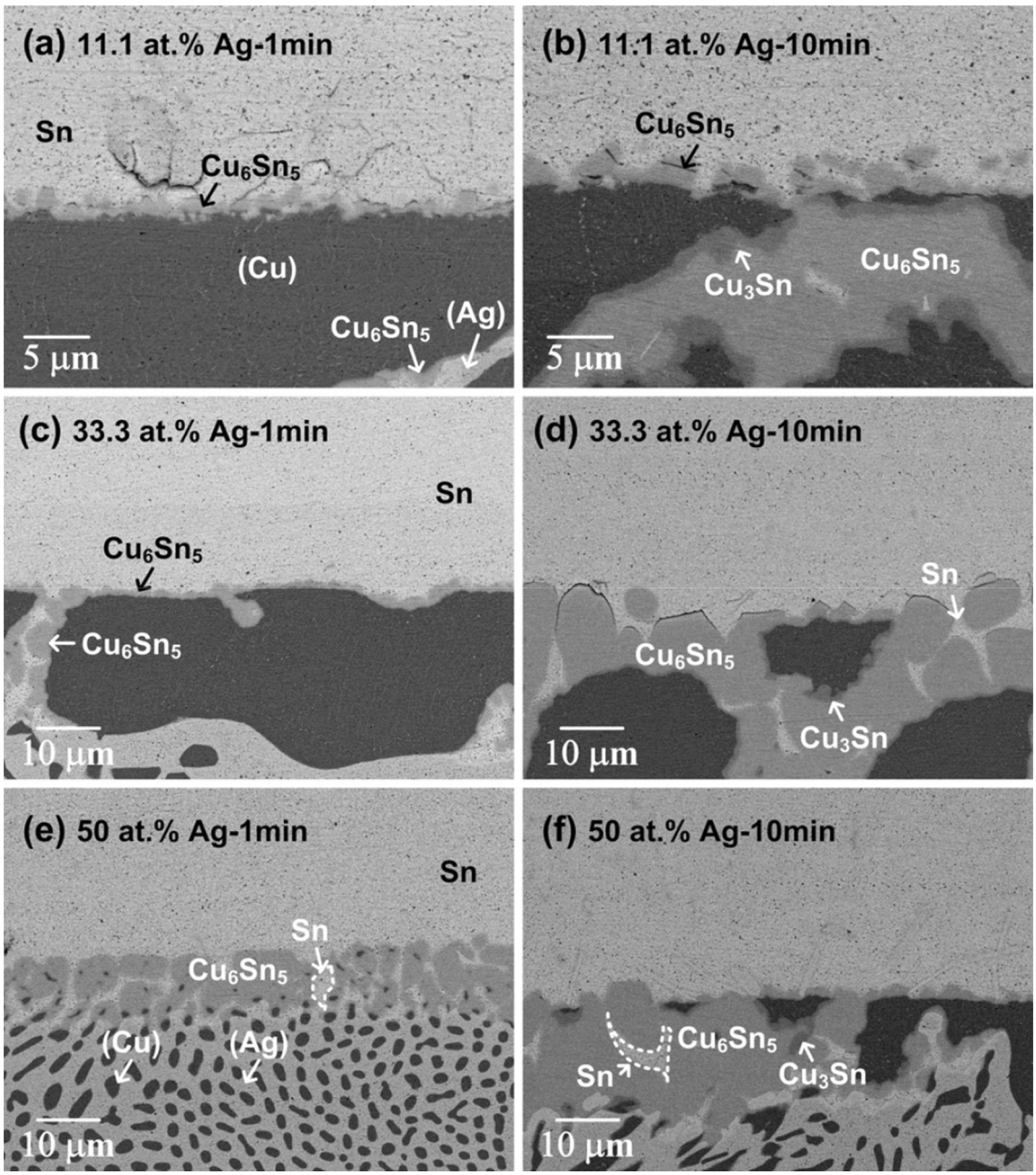

Fig. 2. Cross-sectional SEM micrographs of the interfaces between Sn and various Cu-Ag substrates after liquid/solid reaction at 250°C for 1 min and 10 min: (a, b) Cu-11.1 at.%Ag, (c, d) Cu-33.3 at.%Ag, and (e, f) Cu-50 at.%Ag.

being the (Ag) phase. In addition, the (Cu) phase presented approximately two different grain sizes, as shown in Fig. 1a and b. The larger grains contained the proeutectic (Cu) phase and formed before the eutectic temperature. The smaller grains solidified from the liquid when the temperature decreased below the eutectic temperature and belonged to the eutectic phase. However, the (Cu) grain size differences shown in Fig. 1c were not obvious. These sizes could be similar because the liquidus temperature where the proeutectic (Cu) phase formed was close to the eutectic temperature for the Cu-50 at.%Ag alloy. Therefore, the (Cu) phase in the eutectic structure formed immediately after the proeutectic (Cu) phase, and their grain sizes were difficult to differentiate. According to the Cu-Ag binary phase diagram,[16] the proeutectic (Cu) phase fraction decreases and the eutectic structure increases with increasing Ag content, which is consistent with Fig. 1. Increasing the eutectic fraction simultaneously increased the interphase interface density between the (Cu) and (Ag). The (Cu)/(Ag) interface formed a rapid diffusion pathway for Sn and significantly accelerated the Sn and Cu-Ag alloy interfacial reactions, as discussed below.

Liquid/Solid Interfacial Reactions

Figure 2 shows cross-sectional SEM micrographs for the Sn/Cu-Ag interfaces after the liquid/solid reactions at 250°C. Before discussing the Sn/Cu-Ag interfacial reactions, the conventional Sn/Cu interfacial reaction results are shown for comparison. As shown in Fig. 3, two intermetallic compounds, Cu_6Sn_5 and Cu_3Sn, formed at the Sn/Cu interface after 30 min. The Cu_6Sn_5 phase exhibited a scallop microstructure, while the Cu_3Sn phase was layered. This morphological development of the Cu_6Sn_5 and Cu_3Sn phases is consistent with previous studies.[2,17] In contrast, the Sn/Cu-Ag interfacial microstructure after the liquid/solid reaction was more complicated. Some of the phenomena shown in Fig. 2 are worth discussing. First, Fig. 2a and c shows only 1 min of reaction, and the Cu_6Sn_5 phase formed at both the Sn/Cu-Ag interface and along the (Ag)/(Cu) interface within the Cu-Ag substrates. The Cu_6Sn_5 phase was observed over 20 μm below the Sn/Cu-Ag interface, which indicates that the (Ag)/(Cu) interface acted as a rapid diffusion pathway for Sn. Large amounts of Cu_6Sn_5 phase formed at the (Ag)/(Cu) interface after a 10-min reaction, which significantly consumed the (Ag) and (Cu) phases, as shown in Fig. 2b and d. Second, the growth of the Cu_6Sn_5 phase was much faster along the (Ag)/(Cu) interface than for the interfacial intermetallic phase. Therefore, the Cu-Ag substrates (Fig. 2) were consumed more quickly than the pure Cu substrate (Fig. 3). Third, the Cu_3Sn phase was also observed at the Cu_6Sn_5/(Cu) interface after reaction for 10 min despite having a more sluggish growth rate than the Cu_6Sn_5 phase.

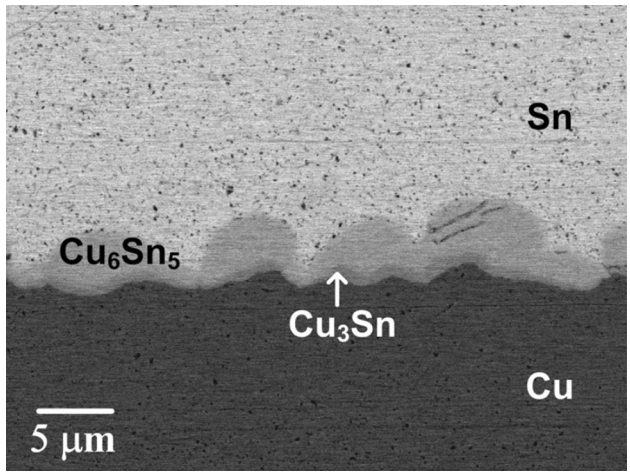

Fig. 3. Cross-sectional SEM micrograph of the Sn/Cu interface after liquid/solid reaction at 250°C for 30 min.

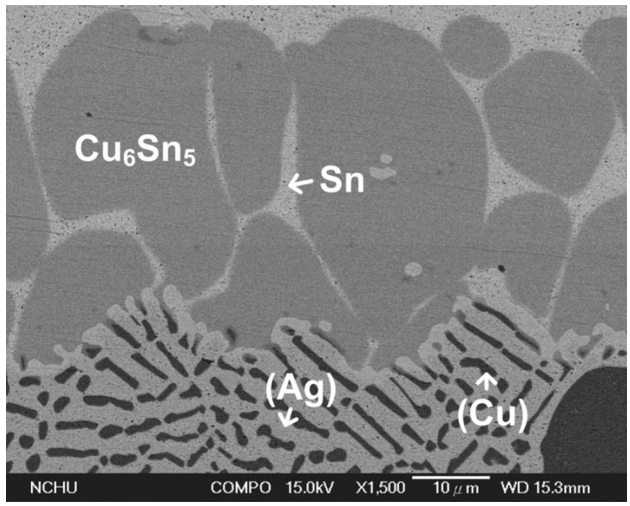

Fig. 4. Cross-sectional SEM micrograph of the Sn/Cu-50 at.%Ag interface after liquid/solid reaction at 250°C for 30 min.

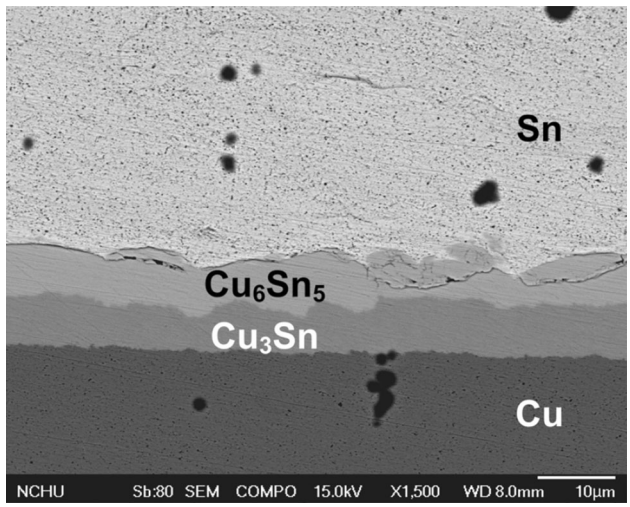

Fig. 5. Cross-sectional SEM micrograph of the Sn/Cu interface after solid/solid reaction at 200°C for 240 h.

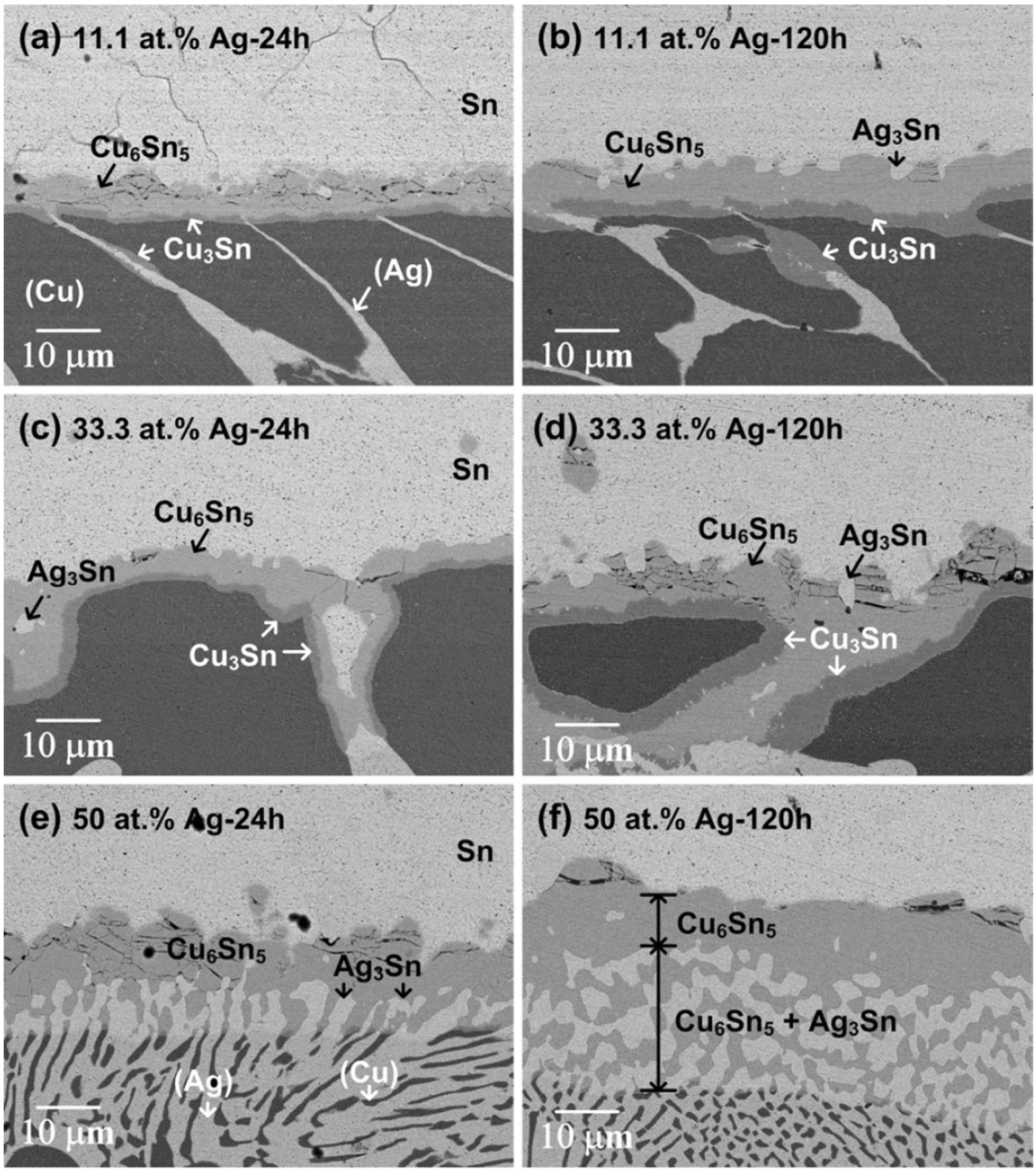

Fig. 6. Cross-sectional SEM micrographs of the interfaces between Sn and various Cu-Ag substrates after solid/solid reaction at 200°C for 24 h and 120 h: (a, b) Cu-11.1 at.%Ag, (c, d) Cu-33.3 at.%Ag, and (e, f) Cu-50 at.%Ag.

Moreover, the growth of the Cu_3Sn phase strongly depended upon the Ag content in the Cu-Ag substrate. Lower Ag content (11.1 at.% and 33.3 at.%) resulted in a uniform Cu_3Sn phase layer that was 1 μm to 2 μm thick along the Cu_6Sn_5/(Cu) interface, as seen in Fig. 2b and d. However, when the Ag content was increased to 50 at.%, the Cu_3Sn phase formed locally at the Cu_6Sn_5/(Cu) interface, as shown in Fig. 2f. For the Sn/Cu-50 at.%Ag interface after reaction for over 30 min, only the Cu_6Sn_5 phase, not the Cu_3Sn phase, was observed, as shown in Fig. 4. These results indicate that increasing the Ag content in the Cu-Ag substrate significantly inhibited the Cu_3Sn phase growth. The Cu_3Sn phase growth is known to be governed by the following reaction[5,11]:

$$9Cu + Cu_6Sn_5 \rightarrow 5Cu_3Sn \quad (1)$$

According to this reaction, Cu_3Sn phase growth is unfavorable for the Sn/Cu-50 at.%Ag system because there is insufficient Cu in the Cu-50 at.%Ag substrate. From a microstructural viewpoint, the (Cu) phase in the Cu-50 at.%Ag substrate was rod shaped and discontinuously dispersed throughout the (Ag) matrix. The surrounding (Ag) phase might

hinder continuous support from the Cu source, which inhibits the Cu_3Sn phase growth.

In addition, the interfacial reaction region shown in Fig. 4 was approximately 40 μm thick and presented a two-phase microstructure consisting of Cu_6Sn_5 and Sn. This interfacial reaction region was much thicker than for the Sn/Cu interface shown in Fig. 3, supporting the significantly enhanced atomic interdiffusion due to the high-density (Ag)/(Cu) interphase interface of the Cu-Ag substrate. The reaction order was as follows: the molten Sn penetrated into the Cu-Ag substrates via the (Ag)/(Cu) interphase interface, dissolved the (Ag) phase, and then reacted with the (Cu) phase to form the Cu_6Sn_5 phase. Figure 4 indicates that the (Cu) phase was surrounded by the (Ag) phase. Therefore, the molten Sn phase must first dissolve the (Ag) phase before contacting the (Cu) phase to form the Cu_6Sn_5 phase, confirming the reaction order described above. The (Cu) phase was eventually completely consumed and transformed into the Cu_6Sn_5 phase. The EDX analysis also confirmed that the Sn phase in Fig. 4 contained small amounts of Ag. Thus, the original (Cu) + (Ag) two-phase microstructure converted into a new Cu_6Sn_5 + Sn two-phase microstructure.

Solid/Solid Interfacial Reactions

As expected, two layers of Cu_6Sn_5 and Cu_3Sn phase formed at the Sn/Cu interface after reaction at 200°C for 240 h, as shown in Fig. 5. However, the interfacial microstructure changed significantly when the Cu substrate was alloyed with Ag. When the Cu-Ag substrate composition was Cu-11.1 at.%Ag or Cu-33.3 at.%Ag, the Cu_6Sn_5 and Cu_3Sn phases not only formed at the Sn/Cu-Ag interface but also penetrated the substrates along the (Ag)/(Cu) interface, as shown in Fig. 6a–d. The growth rate of the intermetallic compounds was much faster for the Cu-33.3 at.%Ag than for the Cu-11.1 at.%Ag substrate. As discussed above, the (Ag)/(Cu) interface formed a rapid diffusion pathway for the Sn. Because the Cu-33.3 at.%Ag substrate possessed higher (Ag)/(Cu) interface density than the Cu-11.1 at.%Ag one, the atomic diffusion and intermetallic compound growth rate were enhanced.

A different and interesting interfacial microstructure was observed when the added Ag content was increased to 50 at.%. As shown in Fig. 6e and f, the interfacial reaction region exhibited a bilayered structure. The top layer next to the Sn contained the Cu_6Sn_5 phase. The bottom layer next to the substrate contained a two-phase microstructure consisting of Cu_6Sn_5 and Ag_3Sn. At the bottom layer and Cu-Ag substrate interface, the Cu_6Sn_5 and Ag_3Sn phases connected directly to the (Cu) and (Ag) phase, respectively. Another phenomenon worth addressing is the differing Sn/Cu-50 at.%Ag interface microstructure after the long-term solid/solid reaction compared with the long-term liquid/solid reaction. As discussed above, the molten Sn dissolved the (Ag) phase, and a Cu_6Sn_5 + Sn two-phase region formed at the liquid/solid interface, as shown in Fig. 4. This result is reasonable because molten Sn can dissolve up to 6 at.% (5.03 wt.%) Ag at 250°C without precipitating the Ag_3Sn phase.[18,19] In contrast, the Ag solubility in solid Sn at 200°C is nearly zero; therefore, the (Ag) phase also reacted with Sn to form the Ag_3Sn phase in conjunction with the Cu_6Sn_5 phase. Increasing the Ag content in the Cu-Ag substrate enhanced the growth rate of these intermetallic compounds (Cu_6Sn_5 and Ag_3Sn) but significantly inhibited the Cu_3Sn phase growth. The Cu_3Sn phase was not observed at the Sn/Cu-50 at.%Ag interface.

CONCLUSIONS

Liquid/solid interfacial reactions between Sn and Cu-*x*Ag substrates at 250°C, where x = 11.1 at.% and 33.3 at.%, formed both Cu_6Sn_5 and Cu_3Sn phases. The Cu_6Sn_5 phase exhibited accelerated growth along the (Ag)/(Cu) interphase interface within the Cu-Ag substrates, which indicated that the (Ag)/(Cu) interface was a rapid diffusion pathway for Sn. The (Ag)/(Cu) interface density increased with increasing Ag content in the Cu-Ag substrate, which enhanced the intermetallic compound growth and Cu-Ag substrate consumption. The Cu_3Sn phase growth was inhibited despite its enhancement on the Cu_6Sn_5 phase growth after adding Ag. No noticeable Cu_3Sn phase was observed at the Sn/Cu-Ag interface after increasing the Ag content to 50 at.%; however, a two-phase (Cu_6Sn_5 + Sn) layer formed. No Ag_3Sn phase was observed, which indicates that the molten Sn reacted only with Cu, forming the Cu-Sn intermetallic compounds, but most likely dissolved the (Ag) phase due to its high solubility. The solid/solid interfacial reactions between Sn and Cu-*x*Ag substrates at 200°C, where x = 11.1 at.% and 33.3 at.%, behaved similarly to the liquid/solid system. However, increase in the Ag content to 50 at.% formed a bilayer at the interface that included a Cu_6Sn_5 phase next to Sn and a two-phase (Cu_6Sn_5 + Ag_3Sn) layer next to the Cu-Ag substrate. This result indicated that the Sn reacted simultaneously with the Cu and Ag at the interface to form the Cu_6Sn_5 and Ag_3Sn phases.

ACKNOWLEDGEMENTS

The authors acknowledge financial support from the National Science Council and Ministry of Economic Affairs, Taiwan, R.O.C. through Grants 101-2221-E-005-076-MY2 and 102-E0605.

REFERENCES

1. M. Abtew and G. Selvaduray, *Mater. Sci. Eng. R* 27, 95–141 (2000).
2. T. Laurila, V. Vuorinen, and J.K. Kivilahti, *Mater. Sci. Eng. R* 49, 1–60 (2005).

3. D.R. Frear, J.W. Jang, J.K. Lin, and C. Zhang, *JOM* 53, 28–33 (2001).
4. C.P. Lin and C.M. Chen, *J. Alloys Compd.* 547, 37–42 (2013).
5. C.P. Lin, C.M. Chen, and Y.W. Yen, *J. Alloys Compd.* 591, 297–303 (2014).
6. C.P. Lin and C.M. Chen, *J. Electron. Mater.* 38, 908–914 (2009).
7. W. Peng, E. Monlevade, and M.E. Marques, *Microelectron. Reliab.* 47, 2161–2168 (2007).
8. C.H. Kuo, H.H. Hua, H.Y. Chan, T.H. Yang, K.S. Lin, and C.E. Ho, *Microelectron. Reliab.* 53, 2012–2017 (2013).
9. C.M.L. Wu, D.Q. Yu, C.M.T. Law, and L. Wang, *Mater. Sci. Eng. R* 44, 1–44 (2004).
10. I.E. Anderson, *J. Mater. Sci.* 18, 55–76 (2007).
11. H.F. Zou, Q.K. Zhang, and Z.F. Zhang, *J. Electron. Mater.* 40, 1542–1548 (2011).
12. H.F. Zou, Q.K. Zhang, and Z.F. Zhang, *Scr. Mater.* 61, 308–311 (2009).
13. C.Y. Yu and J.G. Duh, *J. Mater. Sci.* 47, 6467–6474 (2012).
14. Q.K. Zhang, H.F. Zou, and Z.F. Zhang, *J. Mater. Res.* 25, 303–314 (2010).
15. Q.Q. Lai, L. Zhang, and N. Eustathopoulos, *Acta Mater.* 61, 4127–4134 (2013).
16. J.L. Murray, *Metall. Trans. A* 15, 261–268 (1984).
17. T.Y. Lee, W.J. Choi, K.N. Tu, J.W. Jang, S.M. Kuo, J.K. Lin, D.R. Frear, K. Zeng, and J.K. Kivilahti, *J. Mater. Res.* 17, 291–301 (2002).
18. I. Karakaya and W.T. Thompson, *Bull. Alloy Phase Diagr.* 8, 340–347 (1987).
19. S.K. Seo, S. Kang, D.Y. Shih, and H. Lee, *J. Electron. Mater.* 38, 257–265 (2009).